SCIEPublish

Article

Waterborne Polyurethane Dispersion Synthesized from CO_2 Based Poly(Ethylene Carbonate) Diol with High Performance

Zhenhong Huang, Zonglin He, Chaozhi Wang, Zhu Ding, Jiaoyan Ai, Lina Song *, Baohua Liu *

School of Materials and Energy, Guangdong University of Technology, Guangzhou 510006, China; 1052890325@qq.com (Z.H.); 310251392@qq.com (Z.H.); 474853401@qq.com (C.W.); 1055362823@qq.com (Z.D.); aijy@gdut.edu.cn (J.A.)

* Corresponding authors. E-Mail: songlina@gdut.edu.cn (L.S.); baohua@gdut.edu.cn (B.L.); Tel.: +86-139-2882-8534 (L.S.); +86-185-2012-5150 (B.L.)

Received: 5 December 2022; Accepted: 14 March 2023; Available online: 21 March 2023

Abstract: CO_2-based aliphatic polycarbonates (APCs) are not widely commercialized due to the poor performance and high cost, compared to the traditional synthetic materials. In this paper, poly(ethylene carbonate) diol (PECD) was synthesized from CO_2 and ethylene oxide (EO), and the comprehensive properties were characterized. Furthermore, the preparation and properties of waterborne polyurethane dispersion (WPU) derived from PECD were studied. The result showed that PECD had high reactivity, narrow molecular weight distribution index and excellent thermal stability. The obtained WPU exhibited superior tensile performance, adhesion properties and surface hardness. Due to the low cost of EO and CO_2, PECD is expected to be widely used in the preparation of polyurethanes.

Keywords: Carbon dioxide; Ethylene oxide; Poly(ethylene carbonate) diol; Waterborne polyurethane

1. Introduction

CO_2, as an abundant carbon resource in nature, is an important raw material for the synthesis of chemicals in many industrial fields [1,2]. Using CO_2 to synthesize polymers can reduce the use of the non-renewable petroleum resources, which is, meanwhile, conformed to the concept of carbon neutralization [3–6]. Synthesis and application of aliphatic polycarbonates (APCs) from CO_2 and epoxides were extensively researched over the last 50 years since Inoue's pioneering work [7–11]. However, CO_2-based APCs has not been used on a large scale due to the poor comprehensive properties and high cost, compared to the traditional synthetic materials such as polyethylene, polypropylene, poly-(butyleneadipate-co-terephthalate), etc.

Among CO_2-based APCs, poly(propylene carbonate) diol (PPCD) (Figure 1a) derived from CO_2 and propylene oxide (PO) turned to be a new material for synthesizing polyurethane, and the obtained PPCD-based polyurethane exhibited an outstanding hydrolytic stability and mechanical properties [12–17]. However, compared to poly(propylene glycol) (PPG) and poly(1,4-butylene adipate) diol (PBA), the low reactivity with isocyanate [18] and high production cost of PPCD have limited the further application in polyurethane industry, and hampered the development of carbon neutralization.

The copolymerization of CO_2 and ethylene oxide (EO) was systematically studied [19–22], but the resulting products were non-hydroxyl end-capped high molecular weight polymers, which cannot be used as oligomers in the synthesis of polyurethane. Poly(ethylene carbonate) diol (Figure 1b) (PECD) terminated with the primary hydroxyl groups could be expected to have higher reactivity than PPCD [23]. Similar to the synthesis of PPCD, the preparation of low molecular weight polycarbonate diols and polyols derived from CO_2 and epoxide usually suffered from a low carbonate content, a lack of linear versus cyclic selectivity, and a broad polydispersity index (PDI) [24]. Robson [25] and his co-workers also proposed a detailed mechanism for the preparation of PECD through the ring-opening polymerization of ethylene carbonate (EC). Although PECDs with low molecular weights were successfully prepared, the obtained product had high PDI and low CO_2 utilization. The results of previous studies [26–32] on the synthesis and application of PECD showed that the polyurethane synthesized from PECD exhibited inferior mechanical properties, compared to the polyurethanes derived from conventional commercial diols. Although EO had a great cost advantage over PO, the synthesis and application of PECD were rarely reported, compared to PPCD. Therefore, in this paper, PECD was used to prepare waterborne polyurethane (WPU), which was widely applied in adhesives, coatings, paper and wood products due to the advantages of environmental protection, high efficiency and low toxicity [33–35].

https://doi.org/10.35534/spe.2023.10005

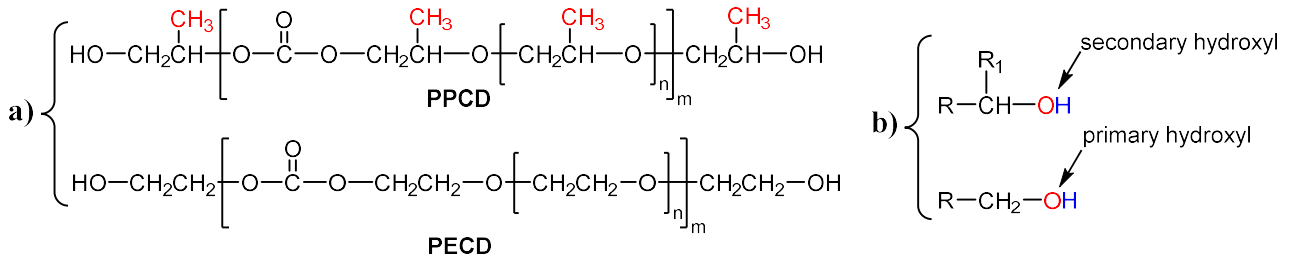

Figure 1. (**a**) Structure of PPCD and PECD, (**b**) Structure of secondary hydroxyl and primary hydroxyl.

In this paper, low molar mass PECD from the copolymerization of CO_2 and EO was characterized, and the feasibility of PECD as a soft segment in the synthesis of WPU was further discussed from the aspects of molecular structure, thermal stability and reactivity. Compared to WPUs used polyester, polyether and polycarbonate diol as the soft segments, WPU synthesized from PECD exhibited excellent mechanical properties and high adhesion. Moreover, the influence of R value ([NCO]/[OH]) and emulsifier content on PECD–WPU was also studied. With the increase of R value, the maximum tensile strength of PECD–WPU reached 63.8 MPa, the elongation at break was 962%, and the pencil hardness was 4H. The successful synthesis of PECD at low cost and its application in polyurethane industry will lead to the application revolution of CO_2-based APCs.

2. Experimental

2.1. Materials

The Co–Zn bimetallic catalyst (Co–Zn DMC) was prepared according to the previously reported method [36]. Poly(ethylene carbonate) diol (PECD, Mn = 2000 g/mol) were synthesized. PECD, poly(propylene carbonate) diol (PPCD, Mn = 2000 g/mol, Guangdong Dazhi Environmental Protection Technology Co., Ltd., Huizhou, China), poly(propylene glycol) (PPG, Mn = 2000 g/mol, Wanhua Chemical Group Co., Ltd., Yantai, China), poly(1,4-butylene adipate) diol (PBA, Mn = 2000 g/mol, Jining Huakai Resin Co., Ltd., Jining, China) and Polycarbonate diol (PCDL, Mn = 2000 g/mol, Jining Huakai Resin Co., Ltd., Jining, China) were dehydrated under vacuum at 110 ℃ for 2 h before use. Isophorone diisocyanate (IPDI) was purchased from Wanhua Chemical Group Co., Ltd. (Yantai, China). Pentaerythritol tetrakis (3-(3,5-di-tert-butyl-4-hydroxyphenyl)propionate) (antioxidant 1010) (94%, Macklin, Shanghai, China), 2,2-bis(hydroxymethyl) propionic acid (DMPA) (98%, Macklin, Shanghai, China) and tin 2-ethylhexanoate (T-9) (95%, Aladdin, Shanghai, China) were used. Triethylamine (TEA, AR) and N,N-dimethylformamide (DMF, AR) were supplied by Tianjin Zhiyuan Chemical Reagent Factory (Tianjin, China). Ethylenediamine (EDA, AR) and acetone (AR) were supplied by Guangzhou Chemical Reagent Factory (Guangzhou, China).

2.2. Preparation of PECD and PECD-WPU

PECD was prepared by the copolymerization of carbon dioxide and ethylene oxide under the catalyst of Co–Zn DMC (Scheme 1), and diethylene glycol (DEG) was used as the molecular weight regulator. Small amounts of antioxidant 1010 was used to reduce the effect of oxygen during the preparation.

The preparation process of PECD–WPU was as follows. PECD, IPDI, DMPA (emulsifier) and DMF were added into a three-neck flask equipped with a mechanical stirrer and a thermometer to react for 30 min at 60 °C under the continuous stirring (400 rpm). T-9 (0.2 wt.% of PECD) was then added into the mixture, and the reaction mixture was heated up to 85 ℃ and reacted for 4 h until NCO reached the theoretical value. The mixture was cooled down, and then an appropriate amount of acetone was added to adjust the viscosity. Then, the mixture was neutralized by TEA at 35 °C for 10 min. After the neutralization, the mixture was poured into cold deionized water and stirred at 2000 rpm for 10 min. EDA was added into the mixture to react for another 1 h below 10 °C. After that, the mixture was slowly heated up to 60 ℃ to remove the acetone to obtain PECD–WPU. PPG–WPU, PBA–WPU, PPCD–WPU and PCDL–WPU were synthesized according to the same process. The chemical structure of different diols and the formula of each emulsion were shown in Figure 2 and Table 1 respectively.

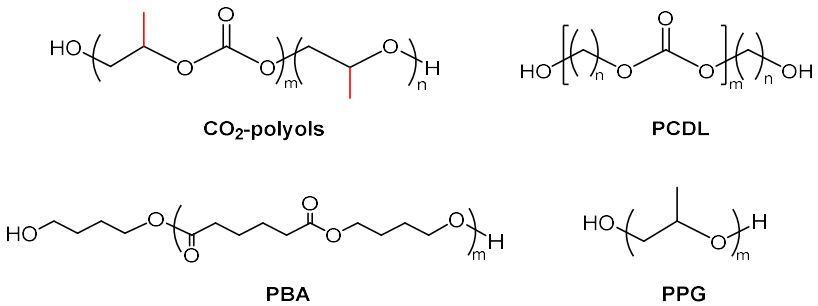

Figure 2. Chemical structures of CO_2-polyols, PCDL, PBA and PPG.

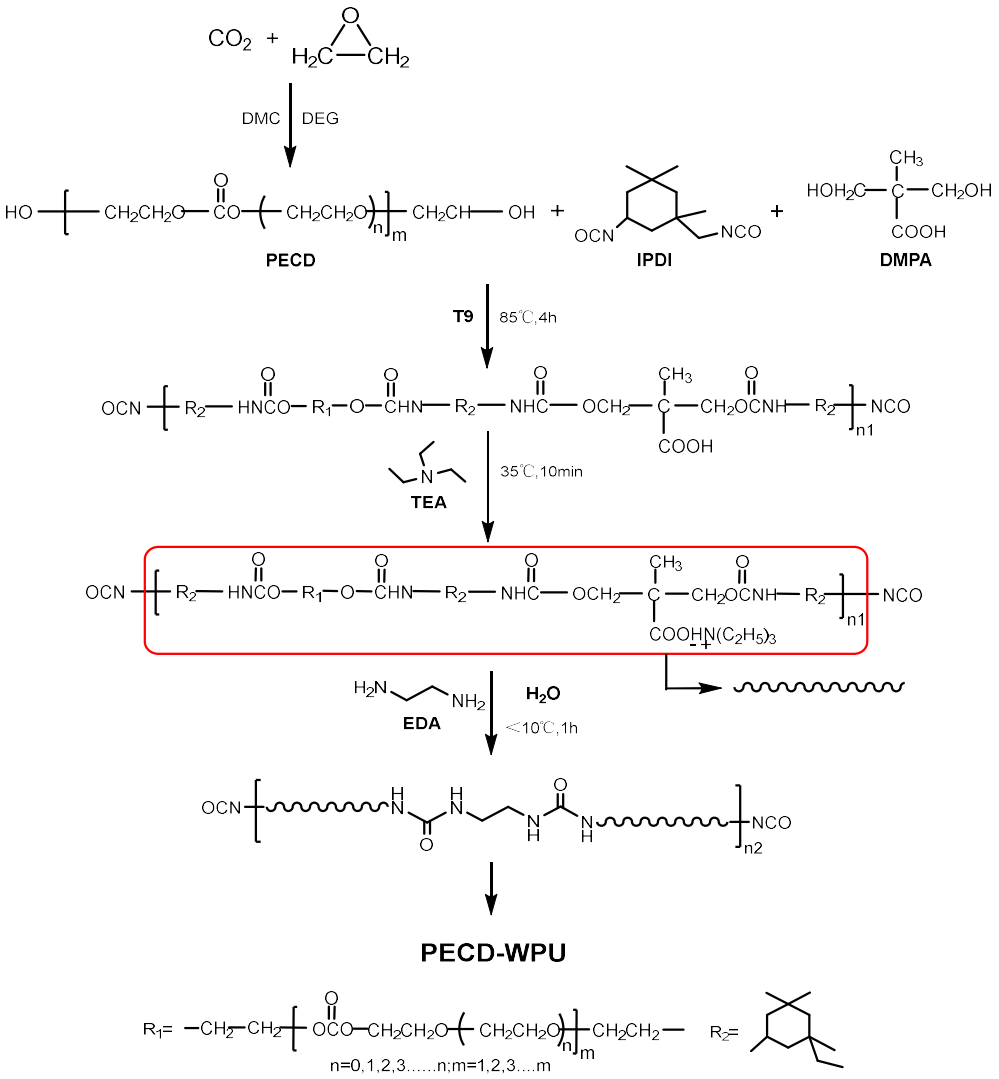

Scheme 1. Reaction route of PECD–WPU.

Table 1. Formulations of WPUs.

Sample	Compositions (g)	R Value [b]	DMPA Content (wt.%)	Hard Segment [c] (%)
PECD-WPU1	PECD/IPDI/DMPA/TEA/EDA(30/7.6/1.82/1.372/0.207)	1.2	4.6	24.30
PECD-WPU2	PECD/IPDI/DMPA/TEA/EDA(30/9.1/1.91/1.44/0.43)	1.4	4.6	27.61
PECD-WPU3	PECD/IPDI/DMPA/TEA/EDA(30/10.6/1.99/1.5/0.656)	1.6	4.6	30.63
PECD-WPU4 [a]	PECD/IPDI/DMPA/TEA/EDA(30/12.2/2.08/1.568/0.896)	1.8	4.6	33.59
PECD-WPU5	PECD/IPDI/DMPA/TEA/EDA(30/13.9/2.17/1.636/1.152)	2.0	4.6	36.47
PECD-WPU6	PECD/IPDI/DMPA/TEA/EDA(30/8.3/1.12/0.844/0.506)	1.6	2.8	24.86
PECD-WPU7	PECD/IPDI/DMPA/TEA/EDA(30/9.0/1.39/1.048/0.556)	1.6	3.4	26.73
PECD-WPU8	PECD/IPDI/DMPA/TEA/EDA(30/9.8/1.69/1.274/0.606)	1.6	4.0	28.74
PECD-WPU9	PECD/IPDI/DMPA/TEA/EDA(30/11.5/2.32/1.749/0.715)	1.6	5.2	32.64

[a] The formulations of PPG-WPU, PBA-WPU, PPCD-WPU and PCDL-WPU are identical to that of PECD-WPU4. [b] Molar ratio of -NCO to -OH in prepolymer. [c] Hard segment content (wt.%) = 100% ($W_1 + W_2 + W_3$)/($W_1 + W_2 + W_3 + W_4$), where W_1: weight of isocyanate, W_2: weight of emulsifier, W_3: weight of chain extender, W_4: weight of polyol.

2.3. Characterization

The composition analyses of WPUs and PECD were performed using a Nicolet6700 Fourier Transform Infrared (FT-IR) Spectrometer (Thermo Fisher Scientific, Waltham, USA) at the range from 500 cm^{-1} to 4000 cm^{-1}. The ^1H NMR spectra were recorded by a Bruker AVANCE III 400 MHz Superconducting Fourier (Bruker, Zurich, Switzerland) using $CDCl_3$ as the solvent.

The crystallinity of PECD and the WPU films were detected by a D/Max-UltimaIV X-ray diffractometer (XRD, Rigaku Corporation, Tokyo, Japan) at room temperature. The 2θ angle was varied from 0° to 70° at a scan speed of 10°/min.

Particle size and distribution were measured by a submicron particle size and Zeta potential analyzer (Delta Nano C, Brookhaven Counter, Inc., New York, USA) at room temperature.

The gel permeation chromatography (GPC) was performed at 35 ℃ on Waters 1515 GPC (Waters, Massachusetts, USA), using polystyrene as the standard and dichloromethane as the eluent.

The hydroxyl value (OHV) of PECD was tested according to ASTM D4274D. The NCO content was measured by titration using dibutylamine-hydrochloric acid as titrant, and it was calculated according to ASTM D2572.

The tensile properties of WPU films were tested by an electro-mechanical universal testing machine (CMT4204, MTS SYSTEMCO., Ltd., Minnesota, USA) at the rate of 200 mm/min according to ASTM D412-1998-2002. The dumbbell-shaped samples with a gauge section with a length and width of 25 mm and 4 mm, respectively, were cut from films with the thickness of 0.5 mm.

Adhesion levels of the coating films to the metallic substrates were tested according to ASTM D3359. The thickness of the coating films was 100 μm. Pencil hardness test of the coating films was set according to ASTM D3363.

The thermal properties of PECD were characterized by thermal gravimetric analysis (TGA) (STA 409 PC, Free State of Bavaria, Germany) under nitrogen atmosphere (flow rate: 50 mL/min) at the heating range from room temperature to 600 ℃. The heating rate was 10 ℃/min.

The glass transition temperature (T_g) of PECD was detected by a differential scanning calorimeter (DSC3, METTLER-TOLEDO, Zurich, Switzerland) under nitrogen atmosphere (flow rate: 30 mL/min). The samples were first heated from −75 °C to 100 °C at a rate of 10 °C/min, and then rapidly quenched to −75 °C. T_g was taken from the second heating curve to minimize thermal history effects.

Solvent absorption testing was performed at room temperature. The WPU films were cut into squares of 2 cm × 2 cm and weighted (m_1). After 24 h immersion in an airtight container containing a solvent (including water, anhydrous ethanol, butanone and toluene, respectively), the films were dried with filter paper and weighted (m_2). The samples were tested three times and the results averaged. The solvent absorption was calculated according to:

$$\text{Solvent absorption (\%)} = \frac{m_2 - m_1}{m_1} \times 100\% \quad (1)$$

The emulsion stability was tested according to the following procedure. The emulsion was placed in a centrifuge tube and centrifuged for 15 min (3000 rpm). A proper amount of emulsion was placed in 55 ℃ bake oven for 7 days. If no precipitation or stratification appeared in either tests, it could be considered that the storage period of emulsion at normal temperature was more than 6 months [17,37].

3. Results and Discussion

Firstly, the prepared PECD was characterized, and the possibility of its application in WPU synthesis was analyzed. The chemical structure of PECD was confirmed by FT-IR, ^{13}C-NMR, and ^{1}H-NMR. From FT-IR spectrum (Figure 3a), two strong absorption peaks at 1750 cm^{-1} and 1265 cm^{-1} were separately attributed to the stretching vibrations of C=O and C–O in the carbonate unit. The absorption peak at 1111 cm^{-1} was assigned to the stretching vibration of C–O–C in the polyether segment. The weak peak at 2954 cm^{-1} was attributed to the methyl groups of catalysts and antioxidant 1010 which were used in the synthesis of PECD. The carbonate and ether units in the structure of PECD were confirmed. The molecular weight obtained by titrating hydroxyl value (calculated by the amount of KOH) was consistent with the result determined by GPC (Figure 3b), proving that PECD was a dihydroxy-terminated oligomer, which can meet the structural requirements for the synthesis of polyurethane.

The structure of PECD was further confirmed by ^{13}C-NMR spectrum (Figure 3d). The chemical shifts at 68.8 ppm and 70.6 ppm were assigned to the ether segment, while the chemical shifts at 65.4 ppm, 67.1 ppm and 154.8 ppm were attributed to the carbonate segment. The preparation of PECD was accompanied by the generation of by-product, EC. From Figure 3c, the signal at 4.54 ppm ($A_{4.5}$) was attributed to CH_2 of EC, indicating the existence of trace EC in PECD. The chemical shifts at 4.25–4.41 ppm ($A_{4.3}$) were assigned to the CH_2 units in the polycarbonate segments, and the chemical shifts at 3.59–3.76 ppm ($A_{3.7}$) were attributed to the CH_2 units in the polyether segments. The molar content of the carbonate unit (F_c) and the weight content (W_{EC}) in PECD could be calculated according to the following equations (2 and 3, respectively). The calculation results showed that F_c and W_{EC} were separately 30% and 0.5wt%.

$$F_c = \frac{A_{4.3}}{2A_{4.3} + A_{3.7}} \times 100\% \quad (2)$$

$$W_{EC} = \frac{88A_{4.5}}{88A_{4.3} + 44A_{3.7} + 88A_{4.5}} \times 100\% \quad (3)$$

The glass transition temperature of PECD was −31.1 °C, which was higher than that of PPCD (−36.8 °C), shown in the DSC curves (Figure 4a). Interestingly, DSC curve of PECD showed a small endothermic melting peak at 31.9 °C, indicating the existence of crystalline structure. It was further evidenced by X-ray diffraction tests. However, PECD and PPCD exhibited similar diffuse scattering peaks at 2θ of approximately 20° in the XRD patterns (Figure 4b), illustrating the poor crystallinity [38]. Due to the more

regular molecular chain structure of PECD [39], the scattering peak of PECD was sharper than that of PPCD, which was in accordance with the DSC results.

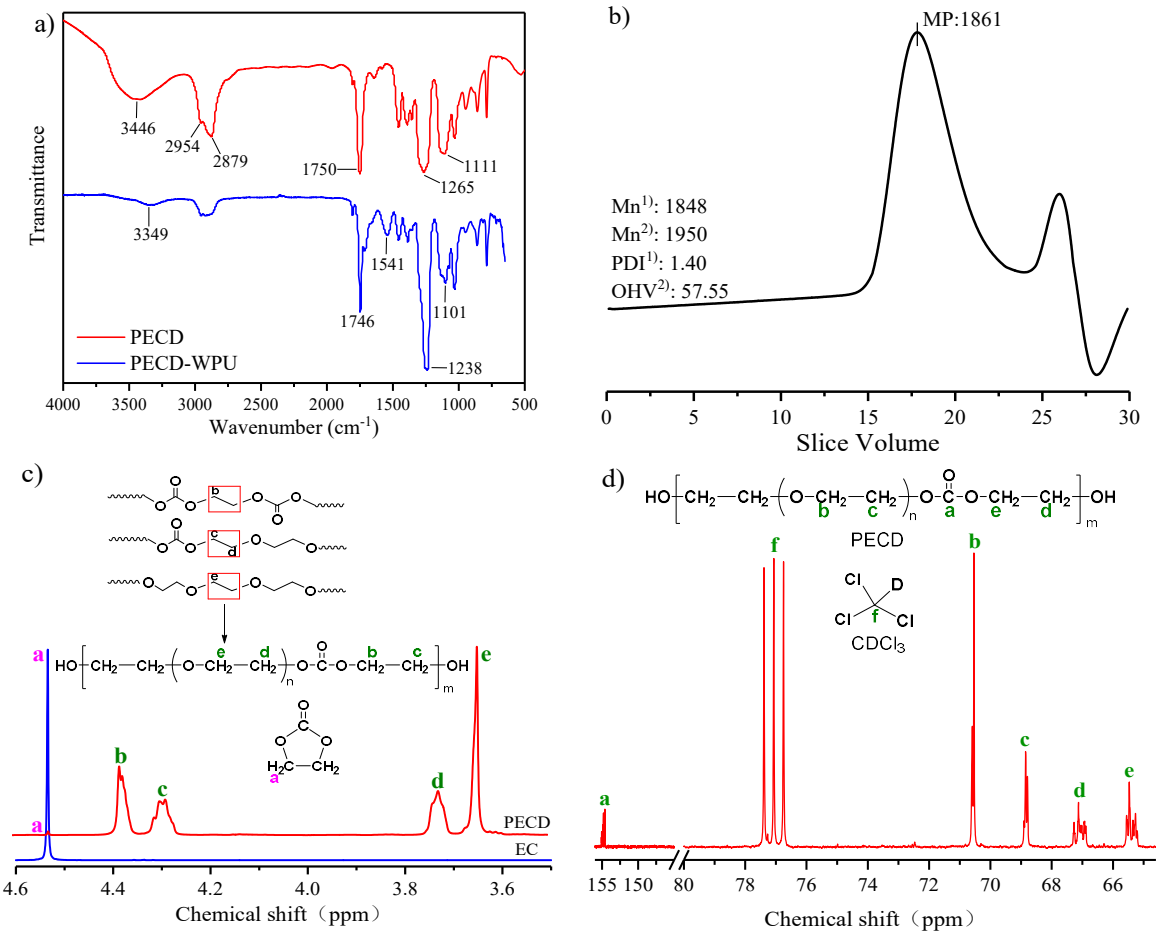

Figure 3. (**a**) FT-IR spectra of PECD (TR, KBr) and PECD–WPU (ATR), (**b**) GPC curve and hydroxyl value of PECD, [1)] calculated by GPC, [2)] determined by the titration method, (**c**) ^{1}H-NMR (400 MHz, $CDCl_3$) spectra of PECD and EC, (**d**) ^{13}C-NMR (400 MHz, $CDCl_3$) spectrum of PECD.

Thermal stability of PECD was characterized by TGA, and the results were showed in Figure 4c. PECD showed two thermal decomposition stages. The initial decomposition temperature of carbonate bonds was varied between 233 °C and 255 °C, corresponding to the first degradation stage from 240 °C to 315 °C in the curves [3]. By the calculation, the peak area of the first thermal degradation stage in DTG curve accounted for about 35% of the total area, which was close to the calculation result of ^{1}H-NMR (F_c = 30%). The second degradation stage from 315 °C to 426 °C could be attributed to the decomposition of the ether bonds [40]. Therefore, PECD was thermally stable in the temperature range of conventional synthesis of WPU (60~120 °C).

Generally, the reactivity of primary hydroxyls with isocyanates was three times stronger than that of the secondary hydroxyls. Part of the terminal hydroxyl structures of PPCD were the secondary hydroxyls, which was ascribed to the side methyl groups in the molecular chains (Figure 1) [18,19]. Therefore, higher reaction temperature and longer reaction time were required to prepare polyurethane using PPCD as the soft segments. Through the reaction of PECD and isophorone diisocyanate (IPDI), the reactivity of PECD was detected by monitoring the variation of the –NCO content in the mixture with the prolongation of time. The reactivities of PPCD, PBA and PCDL were also analyzed under the same reaction conditions, and the results were presented in Figure 4d. Compared to PPCD, PECD exhibited a relatively higher reactivity, which was attributed to the primary hydroxyl groups at the end of the molecular chains. Moreover, the reactivity of PECD was similar to that of PCDL.

PECD–WPU was synthesized by an improved acetone process (Scheme 1), and the FT-IR spectrum (Figure 3a) showed the successful preparation of PECD–WPU. The characteristic peak at 3446 cm^{-1} (O–H stretch) disappeared, and the new characteristic peaks at 3349 cm^{-1} (N–H stretch) and 1541 cm^{-1} (N–H bend) appeared. The disappearance of the characteristic peak at 2270 cm^{-1} indicated the complete reaction of the NCO units. The characteristic peaks of the C=O and C–O stretching vibrations in the O–C=O group appeared at 1746 cm^{-1} and 1238 cm^{-1}. The signal at 1101 cm^{-1} was assigned to be the absorption of SO_3Na [16].

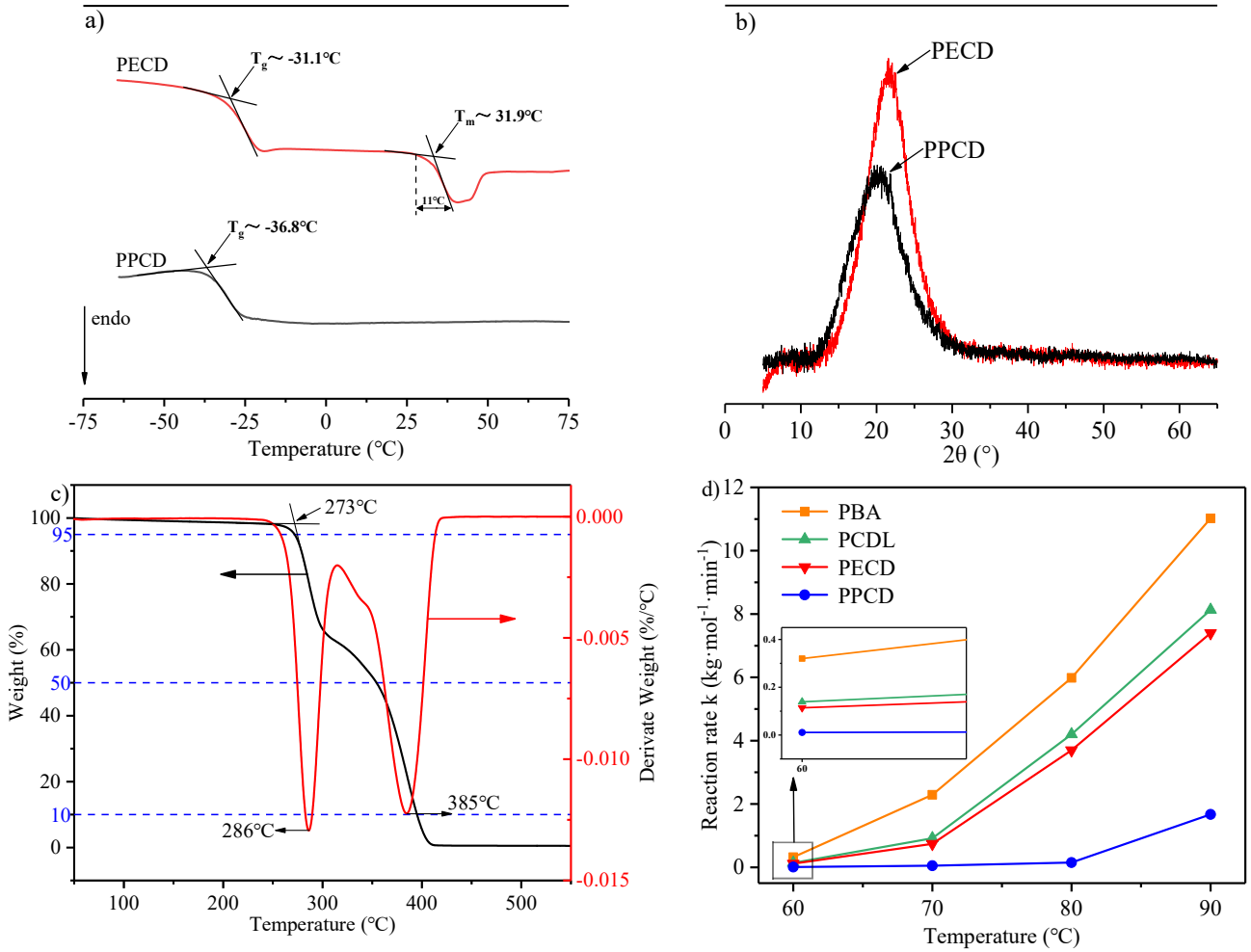

Figure 4. (**a**) DSC curves of PECD and PPCD, (**b**) XRD curves of PECD and PPCD, (**c**) TG and DTG curves of PECD, (**d**) Reactivity of PECD, PBA, PCDL and PPCD at different temperature (n(-NCO)/n(-OH) was 1.021, catalyst addition was 2‰).

Generally, the hard segment content had great influence on the particle size and distribution of WPUs [41–43], so the particle size of PECD–WPU with different R value and DMPA content was tested (Figure 5 and Table 2). As the R value increased, the particle size of emulsion increased and the appearance changed from lucency to white. This could be probably due to the increasing stiffness of prepolymer with the increase of the hard segment content. Furthermore, the increased end distance and volume of the molecular chain resulted in the poor dispersion, so the particle size of the emulsion increased [44]. In addition, the higher R value brought about the more residual –NCO in the mixture which could slowly react with water after the emulsification, resulting in the agglomeration of the emulsion particles and poor emulsion stability. When the R value was 1.2, the emulsion showed significant stratification, which could be attributed to the high molecular weight. Viscosity prepolymer with high molecular weight was difficult to disperse evenly in water [45]. The particle size distributions of PECD–WPUs with different DMPA contents were relatively narrow. The polydispersity index was minimum when the content of DMPA was 3.4%. When the DMPA content was lower than 3.4%, less hydrophilic units and poor dispersity of prepolymer resulted in the increasing particle size [42]. Inversely, the raised DMPA content increased the numbers of the electric double layers, the fluid volume of particles and the viscosity, and further affected the stability of the emulsion [43,45]. Moreover, the elevated hard segment content also increased the viscosity ratio of dispersed phase to continuous phase, which stabilized the dispersed phase and made the emulsion particles easier to aggregate.

The crystallinity of polyurethane mainly depended on the soft segment [16,46], which was further confirmed by this work. Although all XRD curves of WPU films synthesized from different diols (Figure 6a) showed amorphous aggregation state, the WPU film prepared from diol with high crystallinity (such as PCDL) exhibited stronger and sharper diffraction peaks. In addition, the crystallinity of polyurethane increased with the increase of phase separation between hard segment and soft segment [39,46,47], and the phase separation structure had significant effect on the mechanical properties of polyurethane [40].

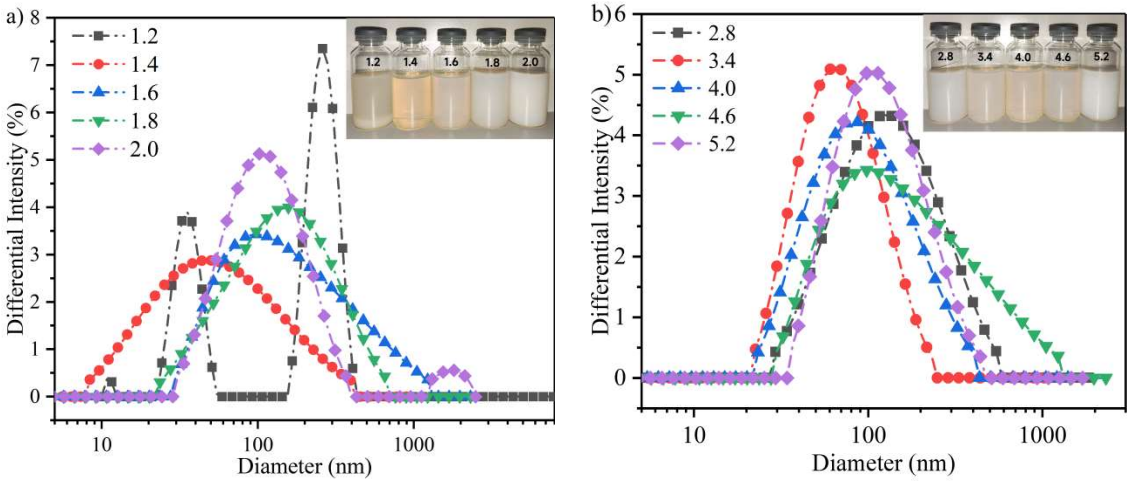

Figure 5. Particle size distribution curves of PECD-WPUs with various R value (**a**) and DMPA content (**b**).

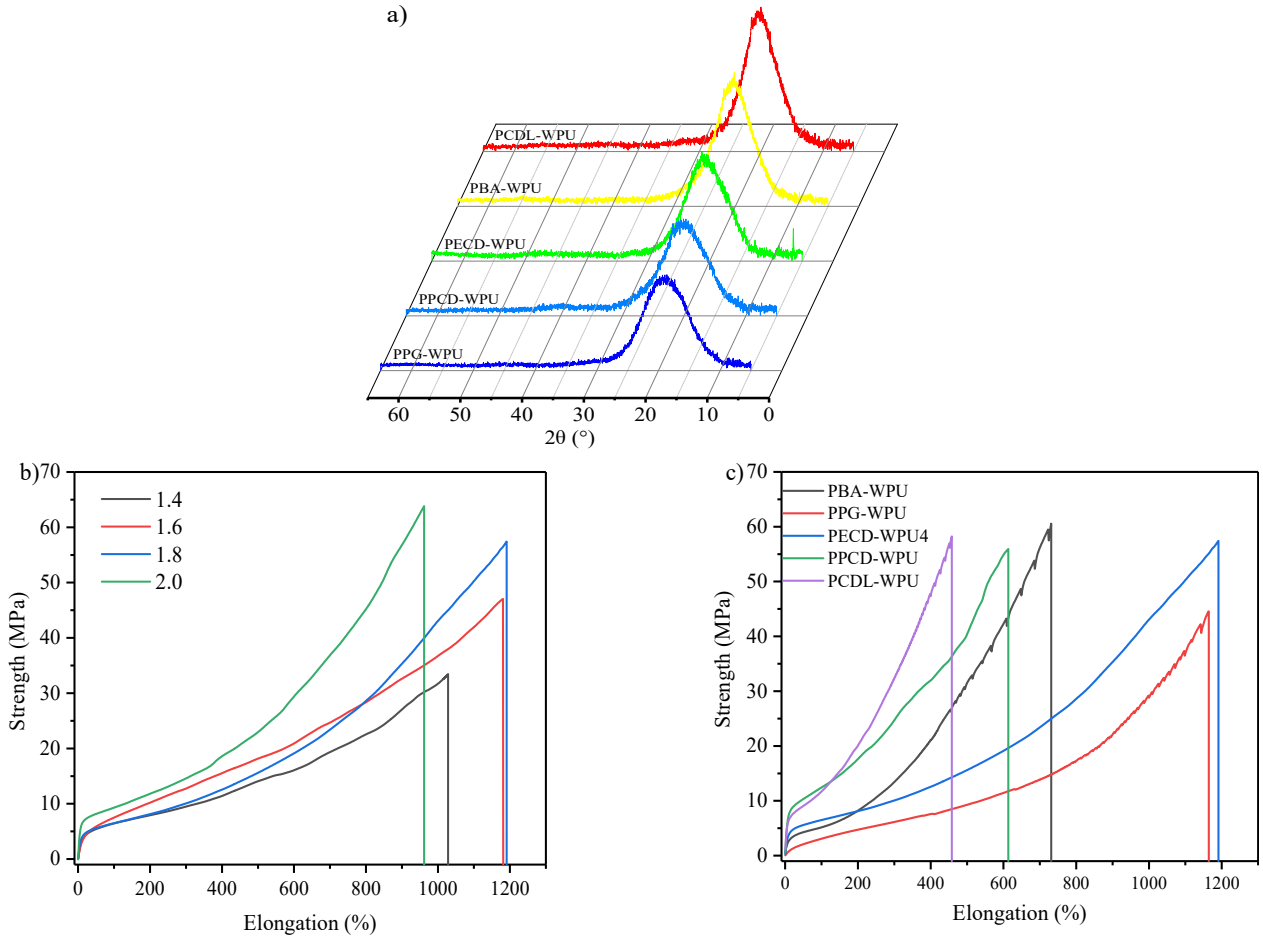

Figure 6. (**a**) XRD patterns of WPUs derived from different soft segments, (**b**,**c**) Stress-strain curves of WPU films with various R values and soft segments.

Table 2. Properties of PECD–WPUs.

Sample	Particle Diameter (nm)	Polydispersity Index	Stability
PECD-WPU1	--	--	Unstable
PECD-WPU2	45.3	0.299	Stable
PECD-WPU3	120.5	0.314	Stable
PECD-WPU4	126.4	0.297	Stable
PECD-WPU5	222.0	0.113	Unstable
PECD-WPU6	107.4	0.262	Stable
PECD-WPU7	63.3	0.232	Stable
PECD-WPU8	77.0	0.253	Stable
PECD-WPU9	101.7	0.210	Unstable

The solvent resistance and mechanical properties of WPU films used different diols as the soft segments were shown in Figure 6b,c and Table 3. It had been reported that PEC was insoluble in toluene [48] and exhibited a typical hydrophilic character like PEO when the carbonate content was low [21]. Therefore, the water absorption value of PECD–WPU film was higher than that of WPUs synthesized from other polyols. The absorption values to anhydrous ethanol and butanone were also high. However, PECD–WPU films showed an excellent resistance to toluene, indicating a possibility of the relatively high polarity of PECD and PECD–WPU, based on the similarity and intermiscibility principle. Although the adsorption values of the PECD–WPU films to water and anhydrous ethanol could be declined by decreasing the DMPA content, the improvement was not enormous. Moreover, the decreased absorption value was also companied by the sacrifice of the mechanical properties.

Table 3. Properties of WPU films prepared from various soft segments.

Sample	Solvent Absorption (%)				Young's Modulus (MPa)	Tensile at Break		Adhesion Level	Hardness
	Water	Anhydrous Ethanol	Butanone	Toluene		Strength (MPa)	Elong (%)		
PECD-WPU2	--	--	--	--	45.9	33.4	1028	5B	HB
PECD-WPU3	82.20	139.70	Broken	28.22	51.2	47.1	1181	5B	2H
PECD-WPU4	86.81	146.29	Broken	26.95	69.3	57.4	1191	5B	3H
PECD-WPU5	--	--	--	--	107.8	63.8	962	5B	4H
PECD-WPU6	40.32	41.39	Broken	31.10	13.7	31.3	1225	5B	1H
PECD-WPU7	44.15	111.74	Broken	30.75	23.8	42.7	1210	5B	1H
PECD-WPU8	54.91	120.12	Broken	28.99	50.7	44.3	1001	5B	2H
PECD-WPU9	111.13	Broken	Broken	26.14	84.2	52.1	931	5B	2H
PPCD-WPU	10.25	Broken	Broken	216.94	124.3	55.9	613	3B	1H
PBA-WPU	7.93	58.39	Broken	131.52	59.7	60.6	731	5B	2H
PPG-WPU	8.70	Broken	Broken	298.53	9.1	44.4	1165	5B	2B
PCDL-WPU	4.70	58.18	Broken	256.70	144.9	58.2	458	2B	2H

The mechanical properties of PECD–WPU films were positively correlated with the content of hard segments. Under the same hard segment content (Table 1), PECD–WPU film showed superior tensile strength close to that of polyester emulsions, and excellent elongation at break comparable to that of polyether emulsions. Compared to the PPCD–WPU film, the elongation at break of PECD–WPU film was higher, which might be due to the increasing hydrogen bonding in the urethane and urea groups of PECD–WPU without the internal rotation and site blocking caused by the side methyl groups. The increasing hydrogen bonding also provided excellent adhesion properties and hardness of the PECD–WPU coatings, which was comparable to the modified PPCD–WPU coatings [15,49]. Wang [50] proposed that the high young's modulus of PPCD–WPU film was due to the rigid carbonate group in the structure (Figure 2), which was also reflected in the PCDL–WPU film. The young's modulus of PECD–WPU film was smaller than that of PPCD–WPU film, due to the superior chain flexibility of PECD.

4. Conclusions

Poly(ethylene carbonate) diol (PECD) derived from ethylene oxide and carbon dioxide was successfully synthesized in our laboratory. The obtained PECD had low molecular weight, narrow polydispersity, excellent thermal stability and high reactivity, also, much lower cost than that of PPCD. WPU synthesized from PECD showed superior tensile strength, toluene resistance and hardness, but the solvent resistance needs to be further improved. Generally, PECD with high reactivity and low cost had potential application in the industrial production of WPU, further, in the other fields of polyurethane production. The synthesis and application of PECD were also beneficial to the immobilization of carbon dioxide and reducing the use of the non-renewable petroleum resources.

Acknowledgments

The authors would like to thank Guangdong Dazhi Environmental Protection Technology Co., Ltd. for providing CO_2-based diols for this work.

Author Contributions

Conceptualization, B.L. and L.S.; Methodology, B.L. and J.A.; Software, Z.H. (Zhenhong Huang); Validation, Z.H. (Zhenhong Huang), Z.H. (Zonglin He) and C.W.; Formal Analysis, Z.H. (Zhenhong Huang) and Z.H. (Zonglin He); Investigation, Z.H. (Zhenhong Huang) and Z.D.; Resources, B.L. and L.S.; Data Curation, Z.H. (Zhenhong Huang); Writing – Original Draft Preparation, Z.H. (Zhenhong Huang); Writing – Review & Editing, B.L. and L.S.; Visualization, Z.H. (Zhenhong Huang) and L.S.; Supervision, B.L. and J.A.; Project Administration, B.L. and L.S.; Funding Acquisition, B.L. and L.S.

Ethics Statement

Not applicable.

Informed Consent Statement

Not applicable.

Funding

The authors declare that they did not receive any funding for this work.

Declaration of Competing Interest

The authors declare no conflict of interest.

Data Availability Statement

The data that support the findings of this study are available from the corresponding author upon reasonable request.

References

1. Langanke J, Wolf A, Hofmann J. Carbon dioxide (CO_2) as sustainable feedstock for polyurethane production. *Green Chem.* **2014**, *16*, 1865–1870.
2. Klaus S, Lehenmeier MW, Anderson CE. Recent advances in CO_2/epoxide copolymerization—New strategies and cooperative mechanisms. *Coord. Chem. Rev.* **2011**, *255*, 1460–1479.
3. Luinstra GA, Borchardt E. Material properties of poly (propylene carbonates). *Adv. Polym. Sci.* **2011**, *245*, 29–48.
4. Luinstra GA. Poly (propylene carbonate), old copolymers of propylene oxide and carbon dioxide with new interests: catalysis and material properties. *Polym. Rev.* **2008**, *48*, 192–219.
5. Welle A, Kroger M, Doring M, Niederer K, Pindel E, Chronakis IS. Electrospun aliphatic polycarbonates as tailored tissue scaffold materials. *Biomaterials* **2007**, *28*, 2211–2219.
6. Zhang J, Qi HX, Wang HJ, Hu P, Ou LL, Guo SH, et al. Engineering of vascular grafts with genetically modified bone marrow mesenchymal stem cells on poly (propylene carbonate) graft. *Artif. Organs* **2010**, *30*, 898–905.
7. Inove S, Konuma H, Tsuruta T. Copolymerization of carbon dioxide and epoxide. *J. Polym. Sci. Part B Polym. Lett.* **1969**, *7*, 287–292.
8. Zhang YY, Wu GP, Darensbourg DJ. CO_2-based block copolymers: Present and future designs. *Trends Chem.* **2020**, *2*, 750–763.
9. Wang YY, Darensbourg DJ. Carbon dioxide-based functional polycarbonates: Metal catalyzed copolymerization of CO_2 and epoxides. *Coord. Chem. Rev.* **2018**, *372*, 85–100.
10. Kozak CM, Ambrose K, Anderson TS. Copolymerization of carbon dioxide and epoxides by metal coordination complexes. *Coord. Chem. Rev.* **2018**, *376*, 565–587.
11. Zhang WB, Fan TW, Yang Z, Yu RP, Zeng XJ, Xu YH, et al. Crystal phase-driven copolymerization of CO_2 and cyclohexene oxide in Prussian blue analogue nanosheets. *Appl. Mater. Today* **2022**, *26*, 101352.
12. Cui SQ, Borgemenke J, Liu Z, Keener HM, Li YB. Innovative sustainable conversion from CO_2 and biodiesel-based crude glycerol waste to bio-based polycarbonates. *J. CO_2 Util.* **2019**, *34*, 198–206.
13. Liu BH. High-performance polycarbonate polyol synthesized from CO_2 goes into commercial operation in Huizhou. *Nat. Gas. Chem. Ind.* **2019**, *44*, 81.
14. Xian WQ, Song LN, Liu BH, Ding HL, Li Z, Cheng MP, et al. Rheological and mechanical properties of thermoplastic polyurethane elastomer derived from CO_2 copolymer diol. *J. Appl. Polym. Sci.* **2018**, *135*, 45974.
15. Ma L, Song LN, Li F, Wang H, Liu BH. Preparation and properties of poly (propylene carbonate)-based waterborne polyurethane-acrylate composite emulsion. *Colloid Polym. Sci.* **2017**, *295*, 2299–2307.
16. Ma L, Song LN, Li F, Wang H, Fan LQ, Liu BH. Synthesis and characterization of poly (propylene carbonate) glycol-based waterborne polyurethane with a high solid content. *Prog. Org. Coat.* **2018**, *122*, 38–44.
17. Xian WQ, Yuan J, Xie ZB, Ou W, Liu XX, Liu BH. Synthesis and properties of CO_2 copolymer-based waterborne polyurethane with high solid content. *J. Polym. Res.* 2021, 28, 254–263.
18. Fu SB, Qin YS, Qiao LJ, Wang XH, Wang FS. Propylene oxide end-capping route to primary hydroxyl group dominated CO_2-polyol. *Polymer* **2018**, *153*, 167–172.
19. Geoffrey WC, Scott A, Tsuyoshi A. Copolymerization of ethylene oxide and carbon dioxide. US Patent 10214614B2, 2019.
20. Jia MC, Zhang DY, Gnanou Y, Feng XS. Surfactant-Emulating Amphiphilic Polycarbonates and Other Functional Polycarbonates through Metal-Free Copolymerization of CO_2 with Ethylene Oxide. *ACS Sustain. Chem. Eng.* **2021**, *9*, 10370–10380.
21. Jeon JY, Lee JJ, Varghese JK, Na SJ, Sujith S, Go MJ, et al. CO_2/ethylene oxide copolymerization and ligand variation for a highly active salen-cobalt(III) complex tethering 4 quaternary ammonium salts. *Dalton Trans.* **2021**, *42*, 9245–9254.
22. Okada A, Kikuchi S, Nakano K, Nishioka K, Nozaki K, Yamada T. New Class of Catalysts for Alternating Copolymerization of Alkylene

Oxide and Carbon Dioxide. *Chem. Lett.* **2010**, *39*, 1066–1068.

23. Ismail TNMT, Palam KDP, Zailan BAB, Soi HS, Kian YS, Abu Hassan H, et al. Urethane-forming reaction kinetics and catalysis of model palm olein polyols: Quantified impact of primary and secondary hydroxyls. *J. Appl. Polym. Sci.* **2016**, *133*, 42955.
24. Naganath GP, Senthil KB, Prakash A, Nikos H, Yves G. Carboxylate Salts as Ideal Initiators for the Metal-Free Copolymerization of CO_2 with Epoxides: Synthesis of Well-Defined Polycarbonates Diols and Polyols. *Macromolecules* **2019**, *52*, 2431.
25. Robson FS, Douglas CH. Polyurethane networks based on poly(ethylene ether carbonate) diols. *Polymer* **1992**, *33*, 2807–2816.
26. Xu SP, Zhang M. Synthesis and characterization of a novel polyurethane elastomer based on CO_2 copolymer. *J. Appl. Polym. Sci.* **2007**, *104*, 3818–3826.
27. Zou XW, Yang SY, Chen LB, Jiang YY. Study on biodegradability of polyurethane based on copolymer of CO_2. *Polyurethane Ind.* **1998**, *13*, 5–7.
28. Harris RF, Joseph MD, Davidson C, Deporter CD, Dais VA. Polyurethane elastomers based on molecular weight advanced poly(ethylene ether carbonate) diols. I. Comparison to commercial diols. *J. Appl. Polym. Sci.* **1990**, *41*, 487–507.
29. Harris RF. Effect of catalyst on the molecular weight advancement of poly(ethylene ether carbonate) polyols. *J. Appl. Polym. Sci.* **1990**, *40*, 1265–1279.
30. Harris RF, Joseph MD, Davidson C. Polyurethane elastomers based on molecular weight advanced poly(ethylene ether carbonate) polyols. IV. Effects of poly(propylene glycol) modified diols. *J. Appl. Polym. Sci.* **1992**, *46*, 1843–1857.
31. Harris RF, Joseph MD, Davidson C, Deporter CD. Polyurethane elastomers based on molecular weight advanced poly(ethylene ether carbonate) polyols. III. Effects of diisocyanate modified diols. *J. Appl. Polym. Sci.* **1991**, *42*, 3241–3253.
32. Storey RF, Hoffman DC. Polyurethane networks based on poly(ethylene ether carbonate) diols. *Polymer* **1992**, *33*, 2807–2816.
33. Barni A, Levi M. Aqueous polyurethane dispersions: A comparative study of polymerization processes. *J. Appl. Polym. Sci.* **2010**, *88*, 716–723.
34. Santamaria-Echart A, Fernandes I, Barreiro F, Corcuera MA, Eceiza A. Advances in Waterborne Polyurethane and Polyurethane-Urea Dispersions and Their Eco-friendly Derivatives: A Review. *Polymers* **2021**, *13*, 409.
35. Vaidya SM, Jadhav SM, Patil MJ, Mestry SU, Mahajan UR, Mhaske ST. Recent developments in waterborne polyurethane dispersions (WPUDs): A mini-review on thermal and mechanical properties improvement. *Polym. Bull.* **2021**, *79*, 5709–5745.
36. Chen S, Hua ZJ, Fang Z, Qi GR. Copolymerization of carbon dioxide and propylene oxide with highly effective zinc hexacyanocobaltate(III)-based coordination catalyst. *Polymer* **2004**, *45*, 6519–6524.
37. Ismoilov K, Akram W, Chauhan S, Ergasheva K, Artikboeva R, Islomova Z, et al. Synthesis and Evaluation of Properties of a Novel Cationic Waterborne Polyurethane Finishing Agent. *J. Chem. Eng. Process Technol.* **2019**, *10*, 398.
38. Zhou X, Fang CQ, Lei WQ, Su J, Li, L, Li Y. Thermal and Crystalline Properties of Waterborne Polyurethane by in situ water reaction process and the potential application as biomaterial. *Prog. Org. Coat.* **2017**, *104*, 1–10.
39. Chen C, Zhang T, Zhou X, Lin HM, Cui JZ, Liu XH, et al. Fluorescent self-healing waterborne polyurethane based on naphthalimide derivatives and its application in anti-counterfeiting. *Prog. Org. Coat.* **2022**, *167*, 106826.
40. Krol P. Synthesis methods, chemical structures and phase structures of linear polyurethanes. Properties and applications of linear polyurethanes in polyurethane elastomers, copolymers and ionomers. *Prog. Mater. Sci.* **2007**, *52*, 915–1015.
41. Garcia-Pacios V, Costa V, Colera M, Martin-Martinez JM. Waterborne polyurethane dispersions obtained with polycarbonate of hexanediol intended for use as coatings. *Prog. Org. Coat.* **2011**, *71*, 136–146.
42. Zhang SB, Lv, HT, Zhang H, Wang B, Xu, YM. Waterborne polyurethanes: Spectroscopy and stability of emulsions. *J. Appl. Polym. Sci.* **2006**, *101*, 597–602.
43. Kim BK, Lee JC. Waterborne polyurethanes and their properties. *J. Polym. Sci. Part A Polym. Chem.* **1996**, *34*, 1095–1104.
44. Garcia-Pacios V, Costa V, Colera M, Martin-Martinez JM. Affect of polydispersity on the properties of waterborne polyurethane dispersions based on polycarbonate polyol. *Int. J. Adhes. Adhes.* **2010**, *30*, 456–465.
45. Perez-Liminana MA, Aran-Ais F, Torro-Palau AM, Orgiles-Barcelo AC, Martin-Martinez JM. Characterization of waterborne polyurethane adhesives containing different amounts of ionic groups. *Int. J. Adhes. Adhes.* **2005**, *25*, 507–517.
46. Naheed S, Zuber M, Barikani M, Salman M. Molecular engineering and morphology of polyurethane elastomers containing various molecular weight of macrodiol. *Mater. Sci. Eng. B* **2021**, *264*, 114960.
47. Hu JL, Mondal S. Structural characterization and mass transfer properties of segmented polyurethane: Influence of block length of hydrophilic segments. *Polym. Int.* **2010**, *54*, 764–771.
48. Fang XG, Yang SY, Chen LB. Synthesis and Biodegradation of Polypropylene ethylene carbonate. *J. Funct. Polym.* **1994**, *7*, 143–147.
49. He ZL, Xian WQ, Ding Z, Wang CZ, Huang ZH, Song LN, et al. Synthesis of novel propylene carbonate diol (PCD) and application in CO_2-based polyols waterborne polyurethane. *J. Polym. Res.* **2022**, *29*, 445.
50. Wang J, Zhang HM, Miao YY, Qiao LJ, Wang XH, Wang FS. Waterborne polyurethanes from CO_2 based polyols with comprehensive hydrolysis/oxidation resistance. *Green Chem.* **2016**, *18*, 524–530.